

An investigation on the use of data-driven scattering profiles in Monte Carlo simulations of ultraviolet light propagation in skin tissues

G V G Baranoski, A Krishnaswamy and B Kimmel

Natural Phenomena Simulation Group, School of Computer Science, University of Waterloo,
200 University Avenue West, Waterloo, Ontario N2L 3G1, Canada

E-mail: gvgsbaran@curumin.math.uwaterloo.ca

Received 5 June 2004, in final form 5 August 2004

Published 1 October 2004

Online at stacks.iop.org/PMB/49/4799

doi:10.1088/0031-9155/49/20/010

Abstract

Ultraviolet light can affect the appearance and medical condition of the human skin by triggering biophysical processes such as erythema, melanogenesis, photoaging and carcinogenesis. The evolution of these processes is related to the amount of ultraviolet light absorbed by skin pigments. This amount may vary with the wavelength and path length of the radiation that is propagated within the skin tissues. For many years, biomedical researchers have been investigating the propagation of ultraviolet light in skin tissues through Monte Carlo simulations. The scattering of the incident radiation by tissue internal structures, a key component in this process, is usually approximated by functions without a plausible connection with the underlying physical phenomena. In this paper, we examine the origins of such an approach, and question its generalized use with respect to wavelengths and biological materials for which there is no supporting data available. Furthermore, we perform comparisons to demonstrate that the accuracy and predictability of Monte Carlo simulations of ultraviolet propagation in skin tissues can be improved by using a data-driven approach to represent the scattering profile of these tissues.

1. Introduction

1.1. Interaction of ultraviolet light with human skin

Skin is a multilayered and inhomogeneous organ, the largest one in the human body. It can be divided into three main sections: stratum corneum, epidermis and dermis. The stratum corneum, a stratified structure composed mainly of dead cells, called corneocytes, embedded

in a particular lipid matrix (Talreja *et al* 2001), is the first and outermost section of human skin. Light absorption is low in this tissue, which is considered by some authors to be part of the epidermis (Tuchin 2000). The absorption in the epidermis is affected by the presence or absence of a natural chromophore, melanin. Melanin is produced by cells called melanocytes occurring in one of the epidermis' constituent layers, the stratum basale, and it is found in membranous particles called melanosomes. According to Pathak and Fitzpatrick (1974), melanin and the distribution of melanosomes in the epidermis are the most important factors in the protection of human skin from the effects of ultraviolet light. The dermis also propagates and absorbs light, and it is primarily composed of dense, irregular connective tissue with nerves and blood vessels.

An understanding of the processes of ultraviolet light propagation in skin tissues is crucial in medical areas, such as dermatology and oncology, since they can affect not only the skin's appearance, but also its health. Ultraviolet light can induce processes such as erythema (an abnormal redness of the skin caused by a dilation of the blood vessels followed by an increase in the volume fraction of blood in the dermal layers), melanogenesis (melanin production) and photoaging (discoloration and wrinkle formation) (Kelfkens and van der Leun 1989, Kollias 1995, van der Leun 1966, Pathak 1995). According to the *Commission Internationale de L'Eclairage* (CIE), ultraviolet radiation can be divided into three regions (Barth *et al* 1999): UV-A (ranging from 315 nm to 380 nm), UV-B (ranging from 280 nm to 315 nm) and UV-C (ranging from 100 nm to 280 nm). The UV-C is mostly absorbed by the ozone layers in the atmosphere. UV-B penetrates deeper than UV-C in skin layers, and it may increase the melanogenesis after a certain period (6–8 h) that follows the erythema reaction (Kollias 1995). UV-A penetrates deeper than UV-B, and it can induce epidermal pigmentation immediately with exposure (Kollias 1995). There are only few exogenous chemical substances that can absorb UV-A efficiently (Stanzl and Zastrow 1995). Commercial tanning beds emit mostly ultraviolet light in the UV-A range. Although the lack of UV-B in infants and small children may lead to disruption of bone growth and increase the probability of tooth decay (Stanzl and Zastrow 1995), overexposure to ultraviolet radiation can induce the formation of melanomas (Fitzpatrick and Bolognia 1995) and carcinomas (Pathak 1995). The former is the most serious form of skin cancer since it presents high metastatic potential and low cure rates (Fitzpatrick and Bolognia 1995). Not surprisingly, a substantial amount of research and resources are applied in the design of superior cosmetics and sunscreens (Stanzl and Zastrow 1995).

1.2. Related work and aims

Computer simulations play a key role in the study of the processes of ultraviolet light interaction with skin tissues. Although different methods may be applied to model light propagation in turbid media such as human skin tissues (e.g., using analytical schemes based on the radiative transfer and Kubelka–Munk theories (Anderson and Parrish 1981, Cotton and Claridge 1996, Diffey 1983, Wan *et al* 1981)), Monte Carlo methods (Metropolis and Ulam 1949) have attracted the attention of many biomedical researchers (Churmakov *et al* 2003, Flock *et al* 1989, Meglinsky and Matcher 2003, Prahl *et al* 1989, Shimada *et al* 2001, Simpson *et al* 1998) since they can provide a flexible, and yet rigorous approach to this problem (Wang *et al* 1995). The core of these Monte Carlo-based simulations is represented by the scattering profile of the particles in the turbid media, which can be represented by a phase function (Prahl 1988).

The outermost layers of human skin, stratum corneum and epidermis, have been the object of extensive analytical and experimental research due to their protective role as an optical

barrier to harmful radiation, especially in the ultraviolet range (Anderson and Parrish 1981, Bruls and van der Leun 1984, Bruls *et al* 1984, Diffey 1983, Everett *et al* 1966). Among these efforts, we highlight the work by Bruls and van der Leun (1984), who performed goniometric measurements of the scattering profile of these tissues. In their paper, Bruls and van der Leun (1984) suggested that the scattering profile of these tissues could be approximated by a single particle phase function, namely the Henyey–Greenstein phase function, henceforth referred to as HGPF, proposed by Henyey and Greenstein to approximate Mie scattering in their study of diffuse radiation in galaxies. It is important to note, however, that the HGPF is neither based on a mechanistic theory of scattering (Jacques *et al* 1987) nor does it have a biological basis.

Later on, Jacques *et al* (1987) followed Bruls and van der Leun's suggestion, and tried to approximate the measured scattering profile of the skin dermis using the HGPF. Yoon *et al* used a similar approach for human aorta. The experiments on dermis and aorta tissues were aimed at specific medical applications and conducted with a HeNe laser (632.8 nm). Motivated by these works, Prahl (1988) proposed a Monte Carlo-based algorithm to model light transport in tissue during laser irradiation. Although a Monte Carlo-based approach was used before to study light propagation in tissue (Wilson and Adam 1983), Prahl's Monte Carlo algorithm, to the best of our knowledge, was the first to incorporate the HGPF to represent the scattering profile of skin tissues.

van Gemert *et al* (1989) also attempted to fit the HGPF to the goniometric measurements performed by Bruls and van der Leun (1984). After that, it was assumed that the HGPF could be used to approximate the scattering profile of organic tissues. In fact, the use of HGPF in analytical and Monte Carlo simulations of light propagation became widespread in many research areas involving tissue optics (Tuchin 2000, Zimnyakov *et al* 2002), and to the best of our knowledge, new comprehensive goniometric measurements of skin subsurface scattering in the ultraviolet range have not been performed, and this generalized use of the HGPF has not been broadly examined in the biomedical literature ever since. Recently, however, accuracy issues started to be addressed. For example, according to Mourant *et al* (1998) the HGPF significantly underestimates the amount of scattering of mammalian cell suspensions at large angles.

In this paper, we investigate practical issues arising from the use of phase functions, such as the HGPF, in simulations of ultraviolet light propagation in skin tissue. First, recall that it has no direct connection with the underlying biophysical phenomena, which negatively affects the predictability of the simulations. Second, as briefly described above, the HGPF was initially meant to be used in skin optics just as a function to fit multiple scattering data measured at specific wavelengths. As we are going to show in the remainder of this paper, the scattering profile approximations using the HGPF deviate from the scattering profile derived from measured data. In short, we believe that the HGPF and its variations cannot be simply generalized and applied to any tissue and any wavelength, and we intend to demonstrate that Monte Carlo simulations of ultraviolet light propagation in skin tissues can be performed with higher accuracy and increased predictability using a data-driven approach to represent the scattering profile of these tissues.

2. Experiments

2.1. Data

In order to determine the accuracy of scattering profiles obtained using the HGPF approximation and a data-driven approach, we compared these profiles with the experimental goniometric data provided by Bruls and van der Leun (1984) for stratum corneum (measured

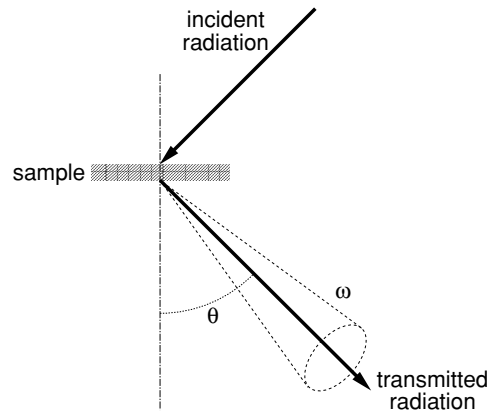


Figure 1. Sketch describing the measurement set up used by Bruls and van der Leun (1984).

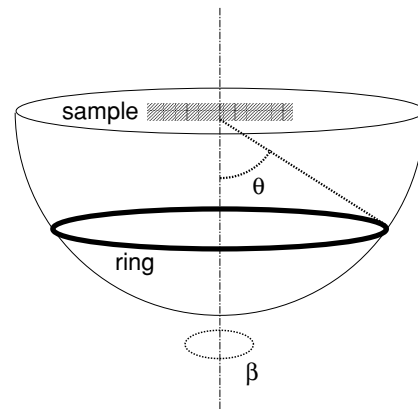


Figure 2. Sketch illustrating the 'ring' approach used by Bruls and van der Leun (1984).

at 254 nm, 302 nm and 365 nm) and epidermis (measured at 302 nm and 365 nm). This experimental data correspond to the amount of radiation transmitted into a solid angle ω centred around the direction given by θ (figure 1), as a fraction of the total radiation transmitted at perpendicular irradiation. In order to determine the contribution that the scattered radiation at a certain polar angle θ makes to the total amount of scattering, Bruls and van der Leun (1984) integrated the scattered radiation over a ring (azimuthal angle β varying from 0° to 360°) of constant θ (figure 2). The measured scattering distributions were in the range given by $0^\circ \leq \theta \leq 62.5^\circ$, and the cumulative fractions of the transmitted radiant flux were expressed as

$$C_i = \frac{\int_{\beta=0^\circ}^{\beta=360^\circ} \int_{\theta=0^\circ}^{\theta=\theta_i+2.5^\circ} I(\beta, \theta) d\omega}{\int_{\beta=0^\circ}^{\beta=360^\circ} \int_{\theta=0^\circ}^{\theta=62.5^\circ} I(\beta, \theta) d\omega} \quad (1)$$

where I represents the transmitted radiant intensity, $d\omega$ corresponds to the differential solid angle (which can be represented by $d\omega = \sin \theta d\theta d\beta$ (Nicodemus *et al* 1992)), and $\theta_i = 5i$ for $i = 0, \dots, 12$.

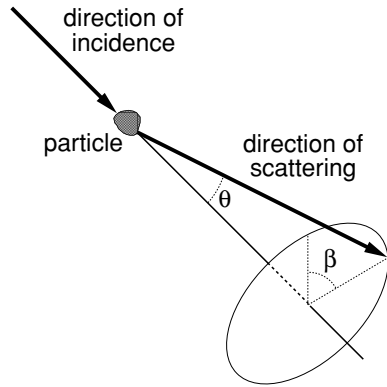


Figure 3. Sketch describing the scattering angles used by the HGPF.

Assuming an azimuthal symmetry of the scattered radiation and solving the integrals with respect to the azimuthal angle β (Bruls and van der Leun 1984), equation (1) simplifies to

$$C_i = \frac{\int_{0^\circ}^{\theta_i+2.5^\circ} I(\theta) \sin \theta \, d\theta}{\int_{0^\circ}^{62.5^\circ} I(\theta) \sin \theta \, d\theta}. \tag{2}$$

The HGPF is given by Henyey and Greenstein (1941):

$$\phi(g, \theta) = \frac{1 - g^2}{(1 + g^2 - 2g \cos \theta)^{\frac{3}{2}}}, \tag{3}$$

where the parameter g , called the asymmetry factor, is defined as the integral over all angles of the phase function multiplied by the cosine of the angle θ . The HGPF is actually a function of *three* parameters: g , θ and β (figure 3). It just happens that an azimuthal symmetry of the phase function is assumed, i.e., the function is constant with respect to the azimuthal angle β . By varying the asymmetry factor in the range $-1 \leq g \leq 1$, it is possible to characterize HGPFs ranging from a completely backward-throwing to a completely forward-throwing form.

For the HGPF asymmetry factors used in our experiments, we considered the values determined by van Gemert *et al* (1989) using a least squares method, which have been commonly used in Monte Carlo scattering simulations. One might argue that the fitting approach used by van Gemert *et al* (1989) to determine the g values could be replaced by another one, which could result into better approximations for the profiles. For this reason, we also used g values obtained by applying a relative error metric to the measured data.

To determine the asymmetry factors, we initially subtracted the consecutive cumulative fractions of the transmitted radiant flux (equation (2)) to get $F_\tau^{(i)} = C_i - C_{i-1}$, for $i = 1, \dots, 12$, and $F_\tau^{(0)} = C_0$. Thus,

$$F_\tau^{(i)} = \frac{\int_{\theta=\max(0^\circ, \theta_i-2.5^\circ)}^{\theta_i+2.5^\circ} I(\theta) \sin \theta \, d\theta}{\int_{\theta=0^\circ}^{\theta=62.5^\circ} I(\theta) \sin \theta \, d\theta}, \tag{4}$$

where $\theta_i = 5i$, for $i = 0, \dots, 12$.

Next, to obtain the HGPF data to be compared to the data from equation (4), we computed the following cumulative density function:

$$P(\theta < \theta') = \int_{\theta=0^\circ}^{\theta=\theta'} \phi(g, \theta) \sin \theta \, d\theta, \tag{5}$$

Table 1. Asymmetry factors obtained by fitting the HGPF to scattering profiles of stratum corneum (measured at 254 nm, 302 nm and 365 nm) and epidermis tissues (measured at 302 nm and 365 nm).

Computation method	Asymmetry factors				
	Stratum corneum			Epidermis	
	254 nm	302 nm	365 nm	302 nm	365 nm
Relative error metric	0.8892	0.8985	0.9107	0.6893	0.7063
Least squares method	0.8858	0.8871	0.8884	0.7076	0.7294

and we obtained

$$C_{g,i} = \frac{P(\theta < \theta_i + 2.5^\circ)}{P(\theta < 62.5^\circ)}, \quad (6)$$

where $\theta_i = 5i$, for $i = 0, \dots, 12$. We then performed the operation $F_\tau^{(g,i)} = C_{g,i} - C_{g,i-1}$ for $i \geq 1$ and $F_\tau^{(g,0)} = C_{g,0}$.

The relative error metric $\epsilon_{\text{rel}}(g)$ used to compare the $F_\tau^{(i)}$ and the $F_\tau^{(g,i)}$, for $i = 0, \dots, 12$, is given by

$$\epsilon_{\text{rel}}(g) = \frac{1}{m} \sum_{i=0}^{m-1} \left| \frac{F_\tau^i - F_\tau^{(g,i)}}{F_\tau^i} \right| \times 100\%, \quad (7)$$

where $m = 13$. We applied the Nelder–Mead simplex search algorithm (Lagarias *et al* 1998) to minimize $\epsilon_{\text{rel}}(g)$ over $g \in [-1, 1]$ to obtain the most suitable asymmetry factor. The asymmetry factors used in our comparisons are presented in table 1.

2.2. Simulation methods

In order to compute the trajectories of the scattered photons using the HGPF (Prahl 1988), a warping function is obtained by setting (Witt 1977)

$$\xi_1 = 2\pi \int_{-1}^{\cos\theta} \phi(g, \cos\theta') d\theta', \quad (8)$$

and finding upon integration that

$$\cos\theta = \frac{1}{2g} \left\{ 1 + g^2 - \left[\frac{1 - g^2}{1 - g + 2g\xi_1} \right]^2 \right\}, \quad (9)$$

where ξ_1 is a uniformly distributed random number on the interval $[0, 1]$. An alternative detailed derivation of such warping function is provided by Baranoski *et al* (2003). For symmetric scattering ($g = 0$), the expression $\cos\theta = 2\xi_1 - 1$ should be used (Prahl *et al* 1989). Since an azimuthal symmetry of the phase function is assumed, the azimuthal angle β can be generated using

$$\beta = 2\pi\xi_2, \quad (10)$$

where ξ_2 is a random number uniformly distributed on the interval $[0, 1]$.

In order to represent the measured scattering profiles using a data-driven approach, we implemented a randomized table look-up algorithm. The scattering angles are stored in a table, whose access indices correspond to the measured fractions of scattered radiation. For each sample (photon), we generate a random number ξ_3 uniformly distributed on the interval $[0, 1]$. We then multiply this number by the table size. The integer part of the resulting value

is used to access the corresponding scattering angle θ stored in the table, which corresponds to the polar scattering angle of the scattered photons. Since an azimuthal symmetry is assumed, the azimuthal angle β of the scattered photons is computed using equation (10).

The table size is limited by the granularity of the measured goniometric data, which consists of values with one decimal digit accuracy. Thus, for each wavelength considered, we used a table with 1000 entries. The intermediate data values were obtained through interpolation, another implementation choice based on the granularity of the measured goniometric data (Bruls and van der Leun 1984). For the sake of simplicity and due to the lack of information about the scattering behaviour between data points, the interpolation scheme consisted in using a first-degree interpolating polynomial (Burden and Faires 1993).

The experiments were performed through the implementation of a virtual goniometer (Krishnaswamy *et al* 2002, 2004), which was used to compute the bidirectional transmittance distribution function (BTDF) associated with the scattering profiles obtained using the HGPF and the randomized table look-up technique. For the computation of each scattering profile, we generate N samples (photons) represented by random numbers uniformly distributed on the interval $[0, 1]$. A value for N is selected such that we can obtain asymptotically convergent results (Krishnaswamy *et al* 2002, 2004). For the experiments present in this paper we used $N = 10^6$. Since the measured data were limited to 62.5° , the scattering angles given by the HGPF beyond this value were discarded to avoid the introduction of bias in our comparisons.

Considering the assumption of azimuthal symmetry of the scattering profiles, the BTDF values were computed on the plane given by the incident light and the tissue's normal. The BTDF values corresponding to the measured data, denoted by f_τ^i , for $i = 0, \dots, 12$, were calculated using

$$f_\tau^i(\omega_i, \omega_t) = \frac{F_\tau^{(i)}}{\omega_t \cos \theta}, \quad (11)$$

where ω_i and ω_t correspond to the incidence and transmissive solid angles. In order to compute the BTDF values corresponding to the HGPF approximation, we replaced $F_\tau^{(i)}$ by $F_\tau^{(g,i)}$ in equation (11). Similarly, to compute the BTDF values corresponding to the data-driven approach, we considered the cumulative fractions $C_{d_i}(\theta)$ (for $i = 0, \dots, 12$) given by the randomized table look-up algorithm, and replaced $F_\tau^{(i)}$ by $F_{d_\tau}^i$ in equation (11), where $F_{d_\tau}^i = C_{d_i} - C_{d_{i-1}}$ for $i \geq 1$ and $F_{d_\tau}^0 = C_{d_0}$.

3. Results and discussion

Figure 4 presents the results of the experiments considering the stratum corneum data. They show noticeable quantitative discrepancies between BTDF values obtained using the data-driven approach and the BTDF values obtained using the HGPF approximation, with a closer agreement to actual BTDF values being obtained using the former. The results of the experiments considering epidermis data, which are presented in figure 5 shows noticeable quantitative and qualitative discrepancies between the BTDF values obtained using the data-driven approach and the BTDF values obtained using the HGPF approximation, with a closer agreement to actual BTDF values being also obtained using the data-driven approach.

The RMS errors presented in table 2 also indicate that by using measured data directly through a data-driven approach one can obtain approximations with a higher degree of accuracy. Regarding the computational costs of each approach, recall that the HGPF formulation includes an expensive fractional exponentiation. For example, for the SGI MIPS R14000 processors used in our experiments, this operation is performed five times slower than a randomized table look-up operation.

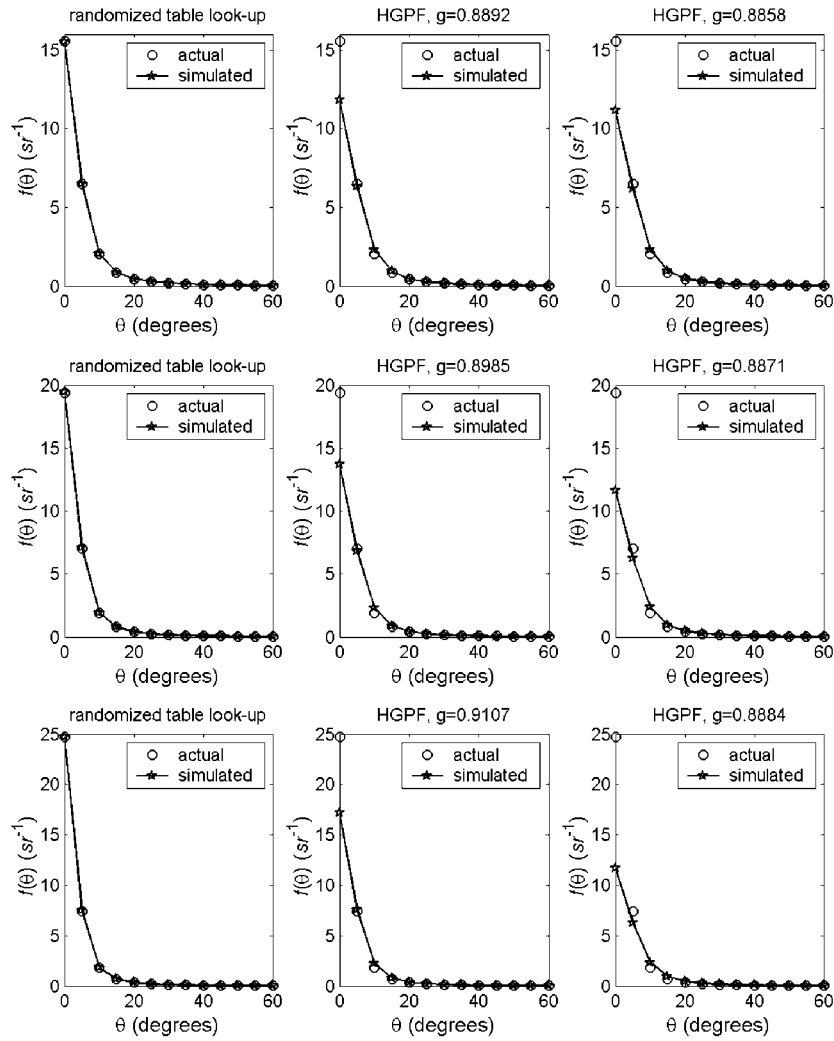


Figure 4. Reconstructed BTDF values for the stratum corneum. Top row: values measured at 254 nm. Middle row: values measured at 302 nm. Bottom row: values measured at 365 nm. Left column: randomized table look-up. Middle column: HGPF (with g given by the relative error metric). Right column: HGPF (with g given by the least squares method (van Gemert *et al* 1989)).

Table 2. RMS errors for the approximation methods with respect to the goniometric measure data for the stratum corneum and epidermis tissues.

Approximation approach	Stratum corneum			Epidermis	
	254 nm	302 nm	365 nm	302 nm	365 nm
HGPF (g given by least squares method)	1.21	2.15	3.24	0.92	0.90
HGPF (g given by relative error metric)	1.06	1.47	1.74	0.65	0.84
Randomized table look-up	0.10	0.12	0.12	0.13	0.12

Due to lack of measured spectral subsurface data, our investigation was limited to few wavelengths. It is worth noting, however, that this data shortage underscores the pitfalls of

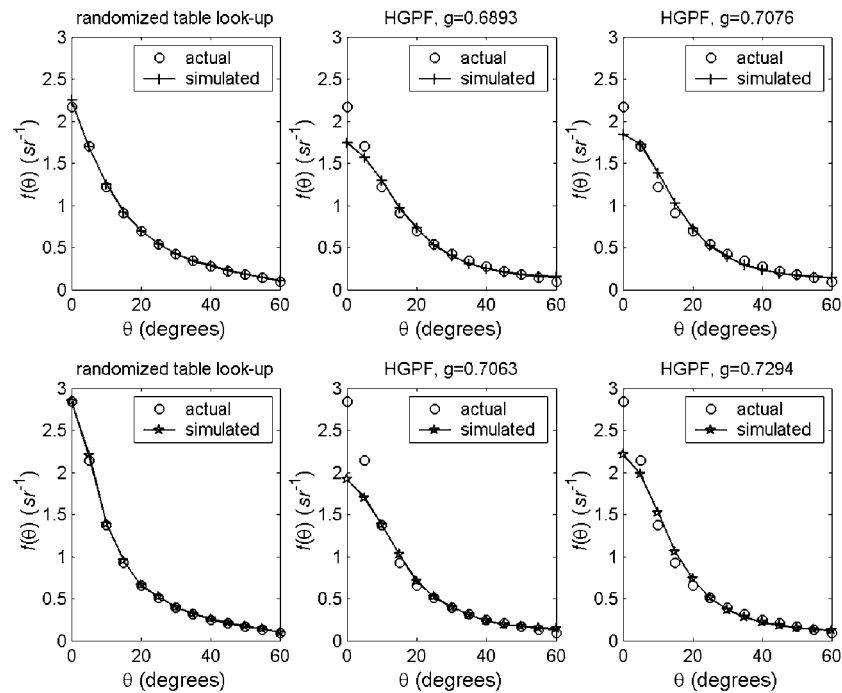


Figure 5. Reconstructed BTDF values for the epidermis. Top row: values measured at 302 nm. Bottom row: values measured at 365 nm. Left column: randomized table look-up. Middle column: HGPF (with g given by the relative error metric). Right column: HGPF (with g given by the least squares method (van Gemert *et al* 1989)).

the generalized use of phase functions such as the HGPF in simulations of ultraviolet light propagation in skin tissues. Considering wavelengths for which there is no measured data available, the selection of asymmetry factors would have neither a biophysical nor an empirical basis.

In order to increase the accuracy of the phase function approximations, one could select another phase function to fit the scattering data (Mourant *et al* 1998), e.g., the Reynolds–McCormick (1980) or the Dunn and Richards-Kortum (1996) phase functions. Another possibility is the use of a multiple-scattered phase function, a concept used by Tessoroff and Wasdon (1994) to simulate multiple scattering in clouds. We remark that the original HGPF formulation represents a single scattering event, and it has been used in tissue optics as a function to fit multiple scattering data. The use of these functions to reconstruct tissue scattering data, however, presents the same limitations found in the HGPF approach, i.e., their parameters are not biologically meaningful, and there are no guarantees with respect to the accuracy of the reconstructed values which may diverge significantly from the data that these functions are trying to fit.

4. Conclusion and future work

Monte Carlo simulations of ultraviolet light propagation in skin tissues aimed at biomedical applications need to satisfy two important requirements, namely accuracy and predictability, in order to provide a sound scientific support to biomedical applications such as noninvasive

optical-tissue diagnostics of physiological and medical skin conditions. The investigation presented in this paper demonstrates that these requirements are more likely to be satisfied by using measured data directly through a data-driven approach, instead of fitting functions that may provide a close qualitative approximation with respect to a wavelength and a poor agreement with data measured at another wavelength. Furthermore, these functions are controlled by parameters that have no biological meaning, and even in the cases where a reasonable fit can be obtained, a data-driven approach has the additional advantage of a smaller computational cost. The application of a data-driven approach in Monte Carlo simulations of ultraviolet light interactions with skin tissues, however, is bounded by data availability. In fact, this aspect emphasizes the increasing need for measured skin data in the ultraviolet range. After all, the reliability of a simulation heavily depends on the availability and quality of supporting data.

Besides the effects on human skin outlined in this paper, ultraviolet light can significantly affect other biological systems (van der Leun and Gruijl 1993). For example, prolonged exposure to ultraviolet light can damage ocular tissues and cause diseases such as cataracts (Taylor *et al* 1998). On land and marine plants (Cullen and Neale 1994), ultraviolet radiation exposure can reduce the rate of photosynthesis, directly affecting plant productivity and biodiversity. As future work, we intend to extend our investigation to these organic materials.

Acknowledgments

The authors would like to thank Dr Wiel A G Bruls and Dr Jan C van der Leun for their valuable feedback on the radiation measurements. Thanks are also due to the anonymous reviewers for their useful comments and suggestions. The work presented in this paper was supported by the Natural Sciences and Engineering Research Council of Canada (NSERC grant 238337) and the Canada Foundation for Innovation (CFI grant 33418).

References

- Anderson R and Parrish J 1981 The optics of human skin *J. Invest. Dermatol.* **77** 13–9
- Baranoski *et al* 2003 Revisiting the foundations of subsurface scattering *Technical Report CS-2003-45* (School of Computer Science, University of Waterloo)
- Barth J *et al* 1999 CIE-134 collection in photobiology and photochemistry *TC6-26 Report: Standardization of the Terms UV-A1, UV-A2 and UV-B* (Commission International de L'Eclairage)
- Bruls W *et al* 1984 Transmission of human epidermis and stratum corneum as a function of thickness in the ultraviolet and visible wavelengths *Photochem. Photobiol.* **40** 485–94
- Bruls W and van der Leun J 1984 Forward scattering properties of human epidermal layers *Photochem. Photobiol.* **40** 231–42
- Burden R and Faires J 1993 *Numerical Analysis* 5th edn (Boston: PWS-KENT Publishing Company)
- Churmakov D *et al* 2003 Analysis of skin tissues spatial fluorescence distribution by the Monte Carlo simulation *J. Phys. D: Appl. Phys.* **36** 1722–8
- Cotton S and Claridge E 1996 Developing a predictive model of skin colouring *Proc. SPIE* **2708** 814–25
- Cullen J and Neale P 1994 Ultraviolet radiation, ozone depletion, and marine photosynthesis *Photosynth. Res.* **39** 303–20
- Diffey B 1983 A mathematical model for ultraviolet optics in skin *Phys. Med. Biol.* **28** 647–57
- Dunn A and Richards-Kortum R 1996 Three-dimensional computation of light scattering from cells *IEEE Sel. Top. Quantum Electron.* **2** 898–905
- Everett M *et al* 1966 Penetration of epidermis by ultraviolet rays *Photochem. Photobiol.* **5** 533–42
- Fitzpatrick T and Bolognia J 1995 Human melanin pigmentation: role in pathogenesis of cutaneous melanoma *Melanin: Its Role in Human Photoprotection* ed M C L Zeise and T Fitzpatrick (Overland Park, KS: Valdenmar Publishing Company) pp 177–82
- Flock S T *et al* 1989 Monte Carlo modeling of light propagation in highly scattering tissues: I. Model predictions and comparison with diffusion theory *IEEE Trans. Biomed. Eng.* **36** 1162–8

- Heney L and Greenstein J 1941 Diffuse radiation in the galaxy *Astrophys. J.* **93** 70–83
- Jacques S *et al* 1987 Angular dependence of HeNe laser light scattering by human dermis *Lasers Life Sci.* **1** 309–33
- Kelfkens G and van der Leun J 1989 Skin temperature changes after irradiation with UVB or UVC: implications for the mechanism underlying ultraviolet erythema *Phys. Med. Biol.* **34** 599–608
- Kollias N 1995 The spectroscopy of human melanin pigmentation *Melanin: Its Role in Human Photoprotection* ed M C L Zeise and T Fitzpatrick (Overland Park, KS: Valdenmar Publishing Company) pp 31–8
- Krishnaswamy A *et al* 2002 Virtual goniophotometric measurements protocol *Technical Report* CS-2002-21 (School of Computer Science, University of Waterloo)
- Krishnaswamy A *et al* 2004 Improving the reliability/cost ratio of goniophotometric measurements *J. Graphics Tools* **9** 31–51
- Lagarias J *et al* 1998 Convergence properties of the Nelder–Mead simplex method in low dimensions *SIAM J. Optimization* **9** 112–47
- Meglinsky I and Matcher S 2003 Computer simulation of the skin reflectance spectra *Comput. Methods Programs Biomed.* **70** 179–86
- Metropolis N and Ulam S 1949 The Monte Carlo method *J. Am. Stat. Assoc.* **44** 335–41
- Mourant J *et al* 1998 Mechanisms of light scattering from biological cells relevant to noninvasive optical-tissue diagnostics *Appl. Opt.* **37** 3586–93
- Nicodemus F *et al* 1992 Geometrical considerations and nomenclature for reflectance *Physics-Based Vision Principles and Practice: Radiometry* ed L Wolff, S Shafer and G Healey (Boston, MA: Jones and Bartlett Publishers) pp 94–145
- Pathak M 1995 Functions of melanin and protection by melanin *Melanin: Its Role in Human Photoprotection* ed M C L Zeise and T Fitzpatrick (Overland Park, KS: Valdenmar Publishing Company) pp 125–34
- Pathak M and Fitzpatrick T 1974 The role of natural photoprotective agents in human skin *Sunlight and Man* ed T Fitzpatrick, M Pathak, L Harber, M Seiji and A Kukita (Tokyo: University of Tokyo Press) pp 725–50
- Prahl S 1988 Light transport in tissue *PhD Thesis* The University of Texas at Austin
- Prahl S *et al* 1989 A Monte Carlo model of light propagation in tissue *SPIE Inst. Ser.* **15** 5 102–11
- Reynolds L and McCormick N 1980 Approximate two-parameter phase function for light scattering *J. Opt. Soc. Am.* **70** 1206
- Shimada M *et al* 2001 Melanin and blood concentration in human skin studied by multiple regression analysis: assessment by Monte Carlo simulation *Phys. Med. Biol.* **46** 2397–406
- Simpson C *et al* 1998 Near infrared optical properties of *ex-vivo* human skin and subcutaneous tissues measured using the Monte Carlo inversion technique *Phys. Med. Biol.* **43** 2465–78
- Stanzl K and Zastrow L 1995 Melanin: an effective photoprotectant against UV-A rays *Melanin: Its Role in Human Photoprotection* ed M C L Zeise and T Fitzpatrick (Overland Park, KS: Valdenmar Publishing Company) pp 59–63
- Talreja P *et al* 2001 Visualization of the lipid barrier and measurement of lipid pathlength in human stratum corneum *AAPS Journal* **3** 1–9
- Taylor H *et al* 1998 Effect of ultraviolet radiation on cataract formation *New Engl. J. Med.* **319** 1429–33
- Tessendorf J and Wilson D 1994 Impact of multiple scattering on simulated infrared cloud sceneimages *SPIE Characterization and Propagation of Sources and Backgrounds* ed P Christensen and D Cohen-Or, pp 75–84 (2223b)
- Tuchin V 2000 *Tissue Optics Light Scattering Methods and Instruments for Medical Diagnosis* (Bellingham, WA: The International Society for Optical Engineering)
- van der Leun J 1966 Ultraviolet Erythema *PhD Thesis* University of Utrecht, The Netherlands
- van der Leun J and Gruijl F 1993 Influences of ozone depletion on human and animal health *UV-B Radiation and Ozone Depletion: Effects on Humans, Animals, Plants Microorganisms, and Materials* ed M Tevini (Boca Raton, FL) pp 95–123
- van Gemert M *et al* 1989 Skin optics *IEEE Trans. Biomed. Eng.* **36** 1146–54
- Wan S *et al* 1981 Analytical modeling for the optical properties of the skin with *in vitro* and *in vivo* applications *Photochem. Photobiol.* **34** 493–9
- Wang L *et al* 1995 MCML—Monte Carlo modelling of light transport in multi-layered tissues' *Comput. Methods Programs Biomed.* **47** 131–46
- Wilson B and Adam G 1983 A Monte Carlo model for the absorption and ux distributions of light in tissue *Med. Phys.* **10** 824–30
- Witt A 1977 Multiple scattering in reflection nebulae: I. A Monte Carlo approach *Astrophys. J. Suppl. Ser.* **15** 1–6
- Yoon G *et al* 1987 Development and application of three-dimensional light distribution model for laser irradiated tissue *IEEE J. Quantum Electron.* **QE-23** 1721–33
- Zimnyakov D *et al* 2002 Speckle technologies for monitoring and imaging of tissues and tissue-like phantoms *Handbook of Optical Biomedical Diagnostics* ed V Tuchin (Bellingham, WA: SPIE Press) pp 987–1036